Proceedings of the 2000 IEEE
International Conference on Robotics & Automation
San Francisco, CA • April 2000

Hugging Walk

Makoto Kaneko, Tatsuya Shirai, and Toshio Tsuji

Industrial and Systems Engineering
Hiroshima University
Kagamiyama, Higashi-Hiroshima 739-8527, JAPAN

Abstract

This paper discusses Hugging Walk (Fig.1) where multiple contacts are allowed between each leg and environment during locomotion. Since an external force can be supported by multiple contact points, legged robots in this style can be expected even more robust against a disturbance (including gravitational force) than those in conventional gaits based on foot contact. The alternative-two-legs-support gait which never exists for conventional gaits based on static balance is introduced. Two indices for stable locomotion are introduced. Experiments are also shown to confirm the basic motion of the proposed gait.
Key words: *Hugging Walk, Enveloping Walk, Legged Robot, Walking Robot, Robustness Index.*

1 Introduction

Legged robots have potential capability to achieve highly intellectual terrain adaptability by cooperational control of the multiple degrees of freedom of the joints. So far, a number of legged robots have been developed in various research institutes[4]-[11]. A number of walking gaits have been studied under the assumption of foot contact, where each foot is allowed to make contact with the environment. In order to maintain a stable locomotion for such a gait, there are two key issues to be considered; one is on slipping between foot and ground (Fig.2(a)), and the other is on falling down due to gravitational force (Fig.2(c)). While a legged robot produces a propelling force through the reaction force between foot and ground during locomotion, the reaction force should be inside of the friction cone at the point of contact to avoid slipping. In case that a legged robot is moving over a horizontal ground under negligible dynamic force, we can easily avoid any slipping motion by designing an appropriate foot trajectory. However, this issue becomes more serious and nonavoidable while it is walking or standing over a ground with a slope. As increasing the angle of slope, for a particular angle q_1, the robot results in the critical situation where a slip occurs between foot and ground. On the other hand, the issue on falling down could happen, even though a robot is walking on a horizontal ground. As for static stability, there is a well-known theorem where the projection of gravitational force should be inside of the support polygon

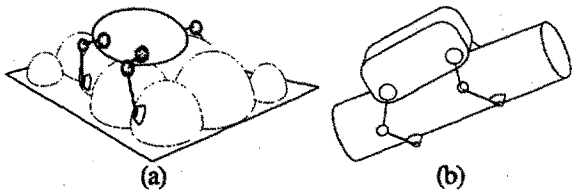

Fig. 1: Example of Hugging Walk

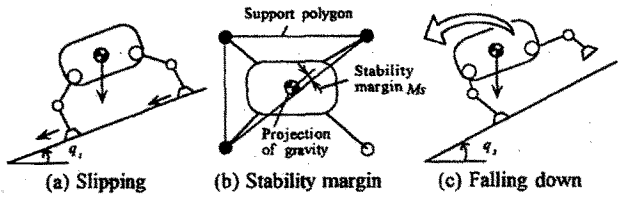

Fig. 2: A legged robot under foot contact

formed by all support legs. Once the projected point is away from the support polygon, the robot necessarily falls down around one edge of the polygon under the hardware where each foot does not equip with any vacuum suction cup. The distance between the point projected by gravitational force and the support polygon is termed as the stability margin M_s which is illustrated in Fig.2(b). While climbing up a terrain with a slope, the margin tends to be small or even zero. Thus, the angle q_2 resulting in the zero stability margin could be another index for a robot climbing up a slope. As a result, $q_{min} = min(q_1, q_2)$ can be an index for keeping a stable locomotion of walking robots, especially when they climb over a terrain with a slope.

Now, suppose an enveloping style as shown in Fig.1, where each leg wraps around an environment. We call this type of walk "*Hugging Walk*". We can expect that q_1 increases drastically under such a walking style and the index q_2 based on stability margin is no more required. As a result, a legged robot can climb up a steeper slope if a hugging style is incorporated. Although such a walk is not efficient from the viewpoints of both energy and speed, it may greatly contribute to extending the working environment of legged robots. This work is motivated by these backgrounds.

This paper first discusses the alternative-two-legs-

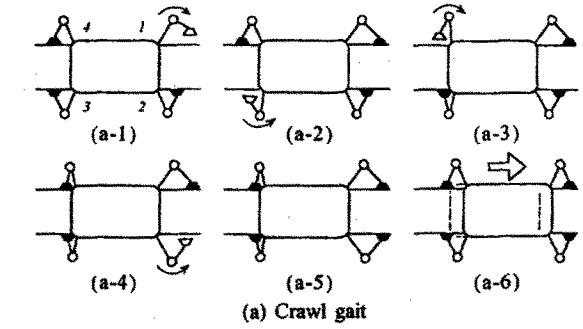

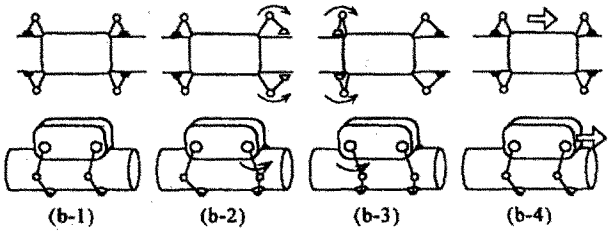

Fig. 3: Example of hugging gait

support gait where front and rear two legs alternatively envelope an environment and produce a propelling force to move the body forward. For such a hugging style, we explain the permissible force boundaries with and without hugging style, and introduce two parameters controlling the stability during locomotion. We demonstrate a hugging walk by using the TITAN-VIII[15] and also confirm the capability for keeping the body without slipping and rotating over a steap slope.

2 Alternative-Two-Legs-Support Gait

Fig.3 shows two examples of hugging gait for a four legged robot, where all legs are initially in support phase. The crawl gait is one of the most popular gaits for legged robots, and it can be also applied to a hugging walk as shown in Fig.3(a), where the one cycle is produced by sequentially swinging the legs 1, 3, 4, and 2, respectively. While more than two support legs are indispensable for keeping a positive stability margin in legged locomotion based on foot contact, this condition is no more required for a hugging walk, since the robot can equivalently produce pulling as well as pushing forces against the gravitational direction by wrapping the environment. As an extreme case, even one leg may produce enough contact forces for supporting the body and for propelling it forward, while it may often encounter an environment where the support leg makes slip due to an insufficient hugging. Let us consider two legs support in which an internal force between two legs can be expected, even under a partial wrapping. Intuitively, the system can resist against an even larger external force under two legs support than under a single leg support. Now, let us further consider three legs support as shown in the crawl gait. Although we can hold more robustness against an external disturbance due to the increase of contact points, the locomotion speed will be drastically down. Unless the environment is steep enough to be difficult to produce a propelling force by the actuators installed, two legs support may provide with a good compromising gait for a hugging walk. This is the reason why we introduce the alternative-two-legs-support gait. The front two legs are first swung forward and wrap the environment, as shown in Fig.3(b-2). The rear two legs then follow the same procedure as shown in Fig.3(b-3). In the next phase, the body is propelled by cooperationally controlling four legs, as shown in Fig.3(b-4). This procedure is repeated continuously. The gait explained in Fig.3(b) is termed as the basic version of the alternative-two-legs-support gait. To increase the locomotion speed, we can modify the basic version, so that the gait may include the body propelling motion synchronously in either front or rear legs swing phase. For such an improved version, of course, more powerful actuators are required than those in the basic version, since the body propelling motion has to be achieved by two legs. We note that the alternative-two-legs-support gait is not available for any static walk based on foot contact where inner link contact is not allowed.

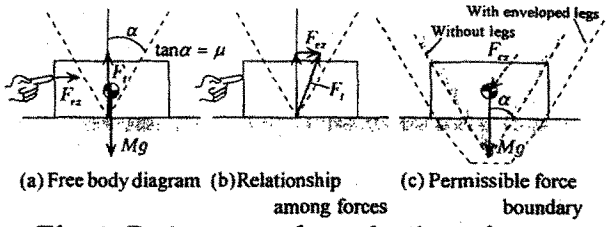

Fig. 4: Basic concept for evaluating robustness

3 Permissible Force Boundary

Before showing two indices, we explain the basic concept behind the idea by using a simple example.

Let us consider a body placed on a table as shown in Fig.4(a), where F_{ex}, F_t, Mg, μ and α denote an external force, reaction force from the table, the gravitational force, friction coefficient and the friction angle satisfying $\tan\alpha = \mu$, respectively. As increasing the external force F_{ex}, the reaction force F_t gradually shifts from the normal direction, as shown in Fig.4(b). When imparting $F_{ex} > Mg\tan\alpha$, F_t can no more exist within the friction cone and the body will inevitably start to slip on the table. In this example, we can evaluate the robustness against an external force by the maximum force where the body can keep stationary. The hatched area in Fig.4(c) denotes the permissible force region where the body can support an external force without any slipping. For example, suppose that an external force as shown by the dotted line is imparted at the center of gravity. As far as such force is included in the hatched region, the body can keep stationary. The permissible force boundary is simply given by the friction cone whose top is placed at the end of the gravitational vector Mg.

Now, let us consider a case where each leg envelopes the table (or environment). Under such a situation, the permissible force boundary will be extended as shown in the dotted line in Fig.4(c). This boundary is determined depending on the contact friction between robot and environment, and on how much torque is imparted to each joint. Generally, the boundary under a hugging style becomes larger than that under a body contact alone. The main discussion hereafter is, therefore, how to find such a boundary under a hugging style. Once we obtain the boundary, we can evaluate the robustness against disturbance by utilizing it.

4 Indices for Stable Locomotion

4.1 Forces and moments acting on the body

Fig.5 shows an example of four legged robot enveloping an environment, where τ and f_{hi} denote the joint torque vector and the force acting at the hip of the body through each leg. For simplifying the discussion, we set the following assumptions:

Assumption 1: Robot has n legs and each leg has m joints.

Assumption 2: Each link has one contact point with environment.

Assumption 3: Mass of link is neglected.

Assumption 4: Frictional coefficient $\mu = \tan\alpha$ is assumed at each contact point.

Assumption 5: Static and dynamic frictional coefficients are not distinguished each other.

Assumption 6: Contact positions are known.

Assumption 7: Small compliance is assumed at each contact point.

Assumption7 is for avoiding the appearance of indeterminate contact force. Since the compliance at contact point is normally unknown, we can not specify the contact force uniquely. Instead, we consider all possible forces for a given set of torques, which is equivalent to considering various kinds of compliance at each contact point.

The relationship between contact force and joint torque for the i-th leg is given by

$$\tau_i = J_i^t f_i \tag{1}$$

where $\tau_i = [\tau_{i1}, ..., \tau_{im}]^t$, $f_i = [f_{i1}^t, ..., f_{im}^t]^t$, and J_i^t denote joint torque vector, contact force vector, and the Jacobian matrix converting the contact force into joint torque. By approximating each friction cone by L faced-polyhedral convex cone, contact force of the i-th leg can be expressed by,

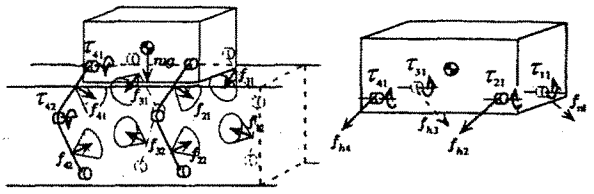

(a) Contact forces between legs and environment

(b) Reaction force and torque

Fig. 5: An example of four legged robot in hugging mode

$$f_{ij} = \sum_{l=1}^{L} \lambda_{ij}^l v_{ij}^l \quad (\lambda_{ij}^l \geq 0) \tag{2}$$

$$= V_{ij}\lambda_{ij} \tag{3}$$

where $V_{ij} = [v_{ij}^1, \cdots, v_{ij}^L] \in R^{3\times L}$, $\lambda_{ij} = [\lambda_{ij}^1, \cdots, \lambda_{ij}^L]^t \in R^{L\times 1}$. This approximation allows us to treat a nonlinear friction constraint as a linear one. For the i-th leg, we obtain the following form.

$$f_i = V_i\lambda_i \tag{4}$$

where $\lambda_i = [\lambda_{i1}^t, \cdots, \lambda_{im}^t]^t \in R^{Lm\times 1}$, and

$$V_i = \begin{bmatrix} V_{i1} & & \mathbf{0} \\ & \ddots & \\ \mathbf{0} & & V_{im} \end{bmatrix} \in R^{3m\times Lm} \tag{5}$$

where v_{ij}^k and λ_{ij}^k denote k-th span vectors of the j-th polyhedral convex cone of the i-th leg and the magnitude of contact force when it lies on the k-th span vector, respectively. From eqs.(1) and (4),

$$\tau_i = J_i^t V_i \lambda_i \tag{6}$$

For all legs,

$$\tau = C\lambda \tag{7}$$

where $\tau = [\tau_1^t, \cdots, \tau_n^t]^t \in R^{mn\times 1}$, $\lambda_i = [\lambda_1^t, \cdots, \lambda_n^t]^t \in R^{Lmn\times 1}$,

$$C = \begin{bmatrix} J_1^t V_1 & & \mathbf{0} \\ & \ddots & \\ \mathbf{0} & & J_n^t V_n \end{bmatrix} \in R^{mn\times Lmn}$$

By solving eq.(7) with respect to, we obtain

$$\lambda = C^\sharp \tau + (I_{Lmn} - C^\sharp C)x \tag{8}$$

where $x \in R^{Lmn\times 1}$ is an arbitrary vector. Since $\lambda \in R^{Lmn\times 1}$ and $\tau = [\tau_1, \cdots, \tau_n]^t \in R^{mn\times 1}$, x has $(L-1)mn$ independent parameters under a full rank matrix C. By considering this, we rewrite eq.(9) as follows

$$\lambda = C^\sharp \tau + N\phi \tag{9}$$

where $\phi \in R^{(L-1)mn\times 1}$ and $N \in R^{Lmn\times(L-1)mn}$ is the row full matrix satisfying $CN = \mathbf{o}$. Finally, the total force f_o for all legs is given by

$$f_o = [I_3, \cdots, I_3] \begin{bmatrix} f_{11} \\ \vdots \\ f_{nm} \end{bmatrix} \quad (10)$$

$$= EV\{C^{\sharp}\tau + N\phi\} \quad (11)$$

where $E = [I_3, \cdots, I_3] \in R^{3\times 3mn}$

$$V = \begin{bmatrix} V_1 & & \mathbf{o} \\ & \ddots & \\ \mathbf{o} & & V_n \end{bmatrix} \in R^{3mn\times Lmn}$$

The total force f_o spans polyhedral convex polygon if each joint torque has upper limit and the contact force is bounded. Under such conditions, the total force corresponding to each vertex in the convex polygon is produced by the contact force lying on one of span vectors of the approximated friction cone. Assuming the contact force on one of span vectors, we can compute one candidate for a vertex. By scanning over all span vectors, we can obtain all candidates for vertices. By connecting each vertex one by one, we can produce the total force set with the convex polygon formed by the outer surface. Therefore, obtaining the total force set is equivalent to finding all vertices of the total force set. In order to take this property, we introduce the following two constraints.

$$S\lambda \geq \mathbf{o} \quad (12)$$

$$S^*\lambda = \mathbf{o} \quad (13)$$

where

$$S = \begin{bmatrix} S_1 & & \mathbf{o} \\ & \ddots & \\ \mathbf{o} & & S_n \end{bmatrix} \quad S^* = \begin{bmatrix} S_1^* & & \mathbf{o} \\ & \ddots & \\ \mathbf{o} & & S_n^* \end{bmatrix} \quad (14)$$

$$S_i = \begin{bmatrix} e_{k1}^t & & \mathbf{o} \\ & \ddots & \\ \mathbf{o} & & e_{km}^t \end{bmatrix} \in R^{m\times mL} \quad (15)$$

$$S_i^* = \begin{bmatrix} \Gamma_1 & & \mathbf{o} \\ & \ddots & \\ \mathbf{o} & & \Gamma_m \end{bmatrix} \in R^{m(L-1)\times mL} \quad (16)$$

$$\Gamma_j = [e_1, \cdots, e_{kj-1}, e_{kj+1}, \cdots, e_L]^t \in R^{(L-1)\times L} \quad (17)$$

$$e_{ki} = [\underbrace{0, \cdots, 0}_{1,\cdots,k_1-i,}, \underbrace{1}_{k_i,}, \underbrace{0, \cdots, 0}_{k_{i+1},\cdots,L}]^t \in R^{L\times 1} \quad (18)$$

Eq.(12) is for keeping each contact force in the pushing direction for the object, and eq.(13) for making each contact force along one of span vector v_{ij}^l. Since S^* and N are column and row full matrices, respectively, S^*N is invertible and as a result, eq.(13) can be solved in the following form if $det(S^*N) \neq 0$.

$$\phi = -D^{-1}S^*C^{\sharp}\tau \quad (19)$$

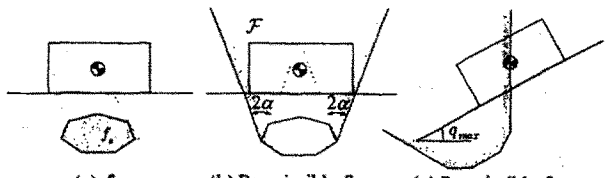

(a) f_s (b) Permissible force boundary(q=0) (c) Permissible force boundary(q=q_{max})

Fig. 6: The relationship between f_s and the permissible force boundary

where

$$D = S^*N \quad (20)$$

Substituting from ϕ into eq(9) and eq(12) yields

$$S\left(I - ND^{-1}S^*\right)C^{\sharp}\tau \geq \mathbf{o} \quad (21)$$

Substituting eq.(19) into eq.(11), we obtain the candidates for vertices of the total force set of the i-th leg in the following form.

$$f_o = EV\left(I - ND^{-1}S^*\right)C^{\sharp}\tau \quad (22)$$

4.2 Deviation of I_f and I_m

In this section, we introduce two indices for evaluating the robustness against a disturbance. Let us now consider the sub total force f_s acted on the body, where f_s is produced by the reaction forces from each leg and the gravity force ($f_s = -f_o + mg$). We note that the reaction force caused by a direct contact between the body and environment is not included in f_s.

For example, suppose f_s is computed, as shown in Fig.6(a). By adding all possible forces produced by the table, we can obtain the permissible force boundary, as shown in Fig.6(b), where $\mathcal{F}$ denotes the permissible force set. As far as the center of gravity exists within the boundary, it is guaranteed that the body can keep stationary, while a local slip may appear at a contact point between leg and environment.

When we incline the environment around an arbitrary axis, we finally reach to a critical situation where $\mathcal{F}$ no more include the origin(the center of gravity). This particular angle is given by $q_{max}(\eta)$, where η is the unit vector expressing the rotational axis. We further examine $q_{max}(\eta)$ for all possible η in the horizontal plane. Thus, we can define an important index I_f,

$$I_f = \min_{0\leq\psi<\pi}(q_{max}) \quad (23)$$

where ψ is the angle denoting the direction of η with respect to the reference frame. The direct meaning of I_f is that the body slip can be avoided irrespective of the choice of η, if the angle of the slope is less than I_f.

Now, let us consider an index I_m expressing the robustness against an external moment. We assume that the body is about to rotate around one edge of the

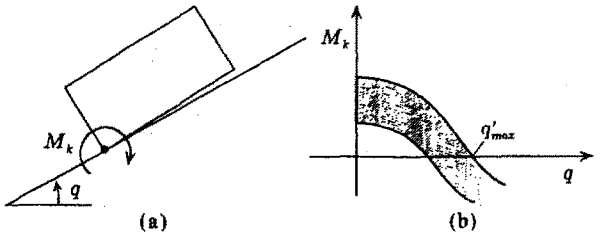

Fig. 7: Moment around the k-th edge

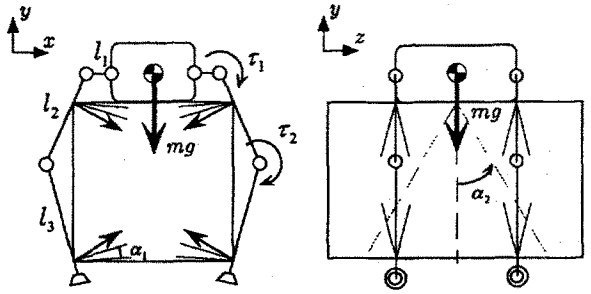

Fig. 8: Simulation model

body as shown in Fig.7(a). This assumption allows us to shift the contact force between the body and the environment on the edge. If the resultant moment around the edge is always produced in such a way that the body rotation can be avoided, we can keep the stability around the edge. The moment around the k-th edge of the body is given by

$$\boldsymbol{M}_k = \sum_{i=1}^{n}\sum_{j=1}^{m} \boldsymbol{r}_{kij} \times (-\boldsymbol{f}_{ij}) + \boldsymbol{r}_{Gk} \times m\boldsymbol{g} \qquad (24)$$

where $\boldsymbol{r}_{kij}$ and $\boldsymbol{r}_{Gk}$ are the position vector from the k-th edge to the j-th contact point of the i-th leg and the position vector from the k-th edge to the center of gravity, respectively. Since $\boldsymbol{f}_{ij}$ generally includes a null space under a given set of torque commands, $\boldsymbol{M}_k$ exists within the band with respect to q, as shown in Fig.7(b). As increasing the slope angle q, $\boldsymbol{M}_k$ finally results in all negative value for a particular inclination angle q'_{max}, which means that the body inevitably rotates the negative direction around the k-th edge when $q > q'_{max}$. Based on these considerations, we define an index concerning rotation as follows,

$$I_m = \min_{k=1,\ldots,K}(q'_{max}) \qquad (25)$$

where K is the number of possible edges for rotating the body. Finally, we evaluate the robustness of a hugging walk by the following index,

$$I_h = min(I_f, I_m) \qquad (26)$$

I_h will be equal to I_f for a legged robot whose center of gravity is located close to the bottom of body, and I_h will coincide with I_m for a robot whose body is extremely high.

4.3 Simulation

Fig.8 shows a simulation model, where $l_1 = 0.07[m]$, $l_2 = 0.23[m]$, $l_3 = 0.3[m]$, $mg = -100.0[N]$, $\alpha_1 =$ 10[*deg*], and $\alpha_2 = 30[deg]$. Fig.9(a) and (b) show simulation results for different torque commands. Since the friction angle between body and environment is $\alpha_2 = 30[deg]$, the body will slip with the inclination angle $q = 30[deg]$, when no reaction force from each leg is influenced on the body. It is interesting to note that I_f is close to 30 when we impart small torque commands to joints. As increasing τ_2 under constant τ_1, I_f increases up to 90[*deg*], which means that the body can support its body even under a tree standing perpendicular to the ground. On the other hand, I_m strongly depends on the position of the center of gravity. Therefore, it depends on the body height, too, as expected.

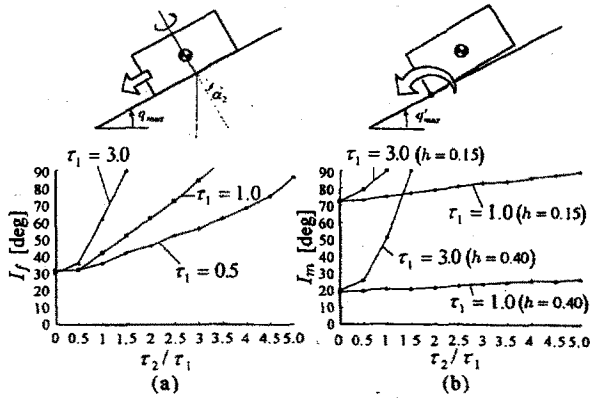

Fig. 9: Simulation results

5 Experimental Approach

We executed various experiments by using the TITAN-VIII developed by Hirose and his group. The TITAN-VIII is a four-legged robot where each leg has three degrees of freedom. The robot is originally designed for walking over an irregular terrain by an appropriate gait based on foot contact, but not for enveloping an environment. Also, since each joint control is based on velocity command, it is not appropriate for a hugging walk requiring joint torque control. In order for the robot to match with a hugging walk, the second link in each leg is covered by compliant material and rubber. This improvement effectively works for avoiding a large contact force between legs and environment, even under a joint velocity based control. Further, we attach a couple of rollers at the bottom of the body, so that we can reduce the contact friction. This mechanical improvement makes it possible to propel the body forward under a hugging style. Fig.10 shows a series of motions while the robot is climbing up a slope under the alternative-two-legs-support gait. Through the test of robustness under an enveloping style, we found that the maximum slope angle without slipping is 61[*deg*] under all legs support phase and 33[*deg*] under two legs support phase, as shown in Fig.11. The maximum slope angle was 20[*deg*] under a conventional gait based on foot contact. Thus, we could confirm that legged robots can extend their working environment under an enveloping style.

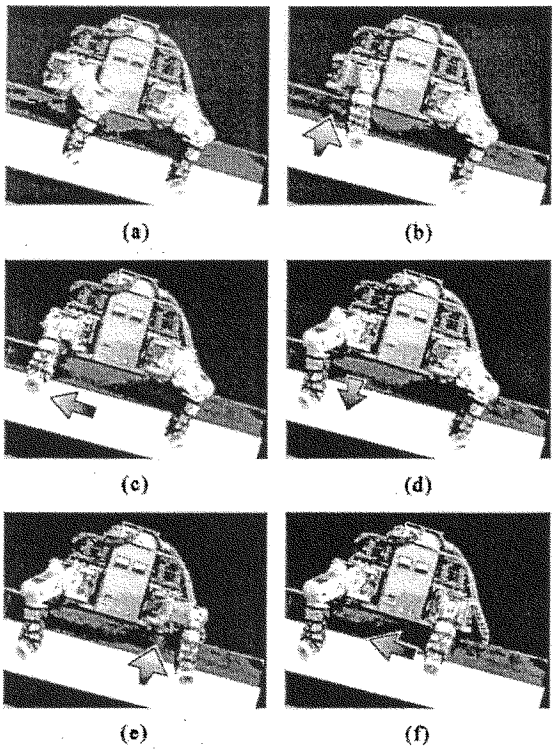

Fig. 10: Hugging walk

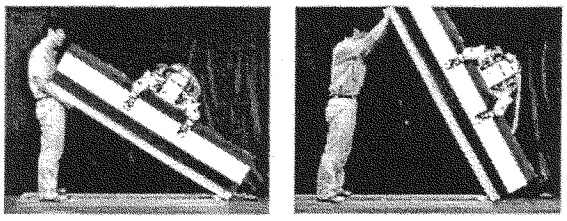

Fig. 11: Test for robustness

6 Conclusions

We discussed hugging walk where multiple contacts are allowed between each leg and environment during locomotion. We introduced two indices for evaluating the robustness against disturbance. By using the TITAN-VIII, we realized the walking motion under a hugging style. We also verified experimentally as well as numerically that the body can sustain against disturbance even more under the hugging gait than under a conventional gaits based on foot contact.

Finally, this work was supported by the Grant-in-Aid for Scientific Research (the Ministry of Education in Japan).

References

[1] A. P. Bessonov and N. W. Umnov: Choice of Geometric Parameters of Walking Machines, *Proc. of ROMANSY'76*, pp.63–74, 1976.

[2] R. B. McGhee: Control of Legged Locomotion System, *Proc. of Eighteenth Joint Automatic Control Conference*, pp.205-215, 1977.

[3] R. B. McGhee, C. S. Chao, V. C. Jaswa and D. E. Orin: Real-Time Computer Control of a Hexapod Vehicle, *Proc. of ROMANSY'78*, pp.323–339, 1978.

[4] M. Russell, Jr: ODEX I: The First Functionoid, *J. of Intelligent Machines*, Vol.5, No.5, pp.12–18, 1983.

[5] I. E. Sutherland: A Walking Robot, *The Marcian Chronicles*, P.O. Box 10209, Pittsburgh, PA. 15232, 1983.

[6] S. M. Song and K. J. Waldron: Machines That Walk: The Adaptive Suspension Vehicle, *MIT Press*, Cambridge, MA, 1989.

[7] E. Rollins, J. Luntz, A. Foessel, B. Shamah and W. Whittaker: Nomad: A Demonstration of the Transforming Chassis, *Proc. of Int. Conf. on Robotics and Automation*, pp.611–617, 1998.

[8] H. Tsukagoshi, K. Yoneda and S. Hirose: TITAN VII: Quarduped Walking and Manipulating Robot on Steep Slope, *Proc. of IEEE Int. Conf. on Robotics and Automation*, pp.494–500, 1997.

[9] S. Kagami, M. Kabasawa, K. Okada, T. Matsuki, Y. Matsumoto, A. Konno, M. Inaba and H. Inoue, Design and Development of a Legged Robot Research Platform JROB-1, *Proc. of IEEE Int. Conf. on Robotics and Automation*, pp.146–151, 1998.

[10] M. Krishna, J. Bares and E. Mutschler, Tethering System Design for Dante II, *Proc. of IEEE Int. Conf. on Robotics and Automation*, pp.1100–1105, 1997.

[11] N. Koyachi, T. Arai, H. Adachi, A. Murakami and K. Kawai, Mechanical Design of Hexapods with Integrated Limb Mechanism: MELMANTIS-1 and MELMANTIS-2,] *Proc. of the 8th Int. Conf. on Advanced Robotics*, pp.273–278, 1997.

[12] A. A. Frank: Automatic Control Systems for Legged Locomotion Machines, *USCEE Report* 273, 1968.

[13] Y. Yu, K. Takeuchi and T. Yoshikawa: Optimization of Robot Hand Power Grasps, *Proc. of IEEE Int. Conf. on Robotics and Automation*, pp.3341-3347(1998).

[14] X. Y. Zhang, Y. Nakamura and K. Yoshimoto: Robustness of Power Grasp, *Proc. of IEEE Int. Conf. on Robotics and Automation*, pp.2828–2835, 1994.

[15] K. Arikawa and S. Hirose: Development of Quadruped Walking Robot TITAN-VIII, *Proc. of International Conference on Intelligent Robots and Systems*, Vol. 1, pp.208–214, 1996.